MOBILE LIDAR MAPPING FOR 3D POINT CLOUD COLLECTION IN URBAN AREAS – A PERFORMANCE TEST

Norbert Haala*[a], Michael Peter[a], Jens Kremer[b], Graham Hunter[c]

[a]Institute for Photogrammetry (ifp), Universitaet Stuttgart, Germany
Geschwister-Scholl-Straße 24D, D-70174 Stuttgart
Forename.Lastname@ifp.uni-stuttgart.de
[b]Ingenieur-Gesellschaft für Interfaces (IGI)
Langenauer Str. 46, D-57223 Kreuztal, Germany
J.Kremer@igi-systems.com
[c]3D Laser Mapping
1A Church Street, Bingham, Nottingham, UK
graham@3Dlasermapping.com

KEY WORDS: Three-dimensional, Point Cloud, Urban, LIDAR, Façade Interpretation

ABSTRACT:

The use of static terrestrial laser scanning for the 3D data capturing of smaller scenes as well as airborne laser scanning from helicopters and fixed wing aircraft for data collection of large areas are well established tools. However, in spite of their general acceptance and wide use both methods have their limitations for projects that include the rapid and cost effective capturing of 3D data from larger street sections. This is especially true if these sections include tunnels or if dense point coverage of the facades of the neighbouring architecture is required. To extend the applicability of laser scanning to these kinds of projects, terrestrial cinematic laser scanning based on mobile mapping systems can be used. Within the paper the components, the workflow and the performance of the vehicle based "StreetMapper" system are described, which simultaneously uses four 2D-laser scanners for 3D data collection, while georeferencing is realised by a high performance GNSS/inertial navigation system. Within our investigations the accuracy of the measured 3D point clouds is determined using reference values from an existing 3D city model. As it will be demonstrated, the achievable accuracy levels of better than 30mm in good GPS conditions make the system practical for many applications in urban mapping.

1. INTRODUCTION

The use of terrestrial laser scanning (TLS) for the collection of high quality 3D urban data has increased tremendously. While urban models are already available for a large number of cities from aerial data like stereo images or airborne LIDAR, TLS is especially useful for accurate three-dimensional mapping of other man-made structures like road details, urban furniture or vegetation. In the context of 3D building reconstruction airborne data collection provides the outline and roof shape of buildings, while terrestrial data collection from ground based views is useful for the geometric refinement of building facades. This is especially required to improve the quality of visualizations from pedestrian viewpoints. However, the complete coverage of spatially complex urban environments by TLS usually requires data collection from multiple viewpoints. This restricts the applicability of static TLS to the 3D data capturing of smaller scenes, which can be captured by a limited number of viewpoints. In contrast, dynamic TLS from a moving platform allows the rapid and cost effective capturing of 3D data from larger street sections including the dense point coverage for the facades of the neighbouring architecture. For this purpose, terrestrial laser scanners are integrated to ground-based mobile mapping systems, which have been actively researched and developed for a number of years (Grejner-Brzezinska et al 2004). While multiple video or digital cameras have been traditionally used by these systems for tasks like highway surveying, their applicability has been increased considerably by the integration of laser scanners.

Within this presentation, the performance and accuracy of the mobile mapping system "StreetMapper", the first commercially available fully integrated vehicle based laser scanning system will be discussed. The StreetMapper mobile laser scanning system was developed initially to fill a demand for measurement and recording of highway assets (Kremer & Hunter 2007). The system uses four 2D laser scanners integrated with a high performance GNSS/inertial navigation system. By these means a dense and area covering collection of georeferenced 3D point clouds is feasible. The main interest of our investigations is the evaluation of data quality for points measured at building facades. Firstly, buildings are the main objects of interest if mobile LIDAR mapping is applied for 3D point cloud collection in urban areas. Secondly, the use of vertical building faces as references surfaces complements the investigations presented by (Barber et al 2008). There, an approximate planimetric accuracy of 0.1 m of the StreetMapper system could be proven for the measurement of street surfaces. However, these investigations were mainly limited to the downward looking laser sensor scanning the road surface at relatively short ranges around 4 to

* Corresponding author

5 m. In contrast, our studies are based on 3D point clouds collected by all scanners of the systems measuring at a variety of ranges.

After a brief description of the components and the theoretical accuracy potential of the StreetMapper system in the following section, the collection of the test data is discussed in section 3. Section 4 covers the presentation and interpretation of our accuracy investigations, while the final discussion in section 5 will conclude the paper.

2. STREETMAPPER SYSTEM

The StreetMapper mobile laser scanning system collects 3D point clouds at a full 360° field of view by operating four 2D-laser scanners simultaneously. The system is easily deployed on a range of different vehicles and the first StreetMapper system has been operating since early 2005.

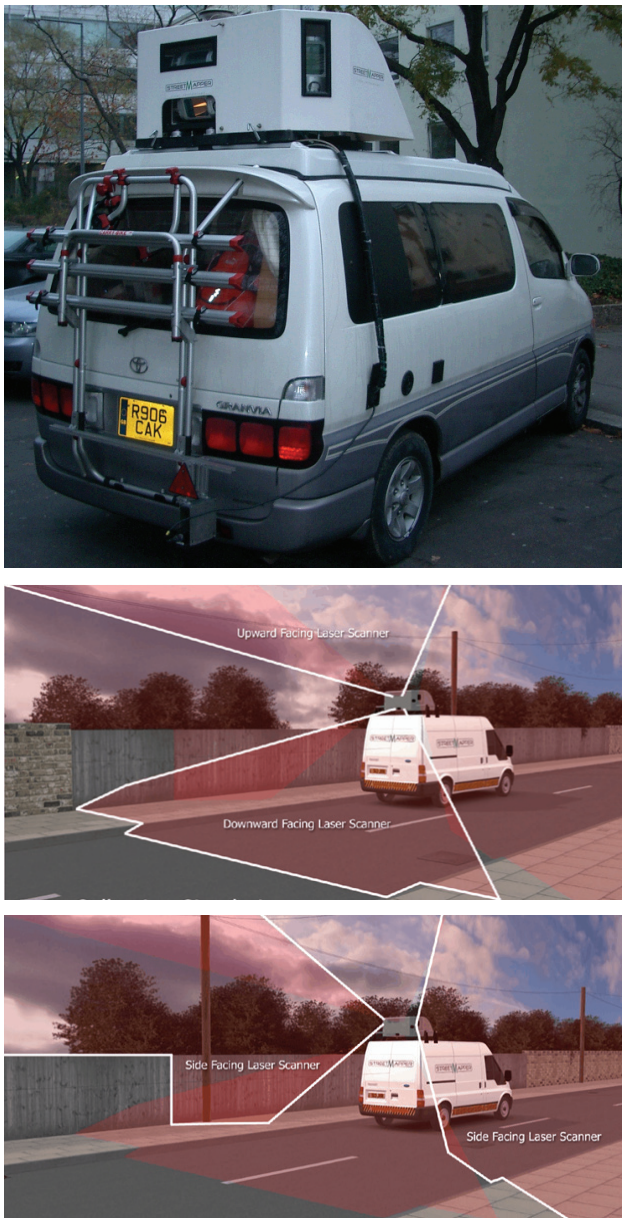

Figure 1: Configuration of the Streetmapper system.

Figure 1 depicts the configuration of the system with the four 2D scanners. The mounting position and angles aim to provide maximum coverage with some overlapping data between each adjacent scanner for calibration purposes. All scanners were manufactured by Riegl Laser Measurement Systems, Horn, Austria. In our test configuration, two Q120i profilers provide the upward and downward looking view at a mounting angle of 20° from the horizontal, respectively. Nominally, the Q120i has maximum range of 150 m at an accuracy of 20 mm. The side facing view to the left (with respect to the driving direction) is generated by a Q140 instrument. The respective scans to the right are measured by a Q120. The mounting angle for both of the side facing instruments is 45°. All four scanners were operated at a maximum scan angle of 80°. Positioning and orientation of the sensor platform is realised by integration of observations from GNSS (Global Navigation Satellite Systems) and Inertial Measurement Units (IMU). For this purpose the TERRAcontrol system from IGI, Germany is used. A more detailed presentation of the components of the TERRAcontrol system will be given together with the achievable georeferencing accuracies in section 4.1, followed by a discussion of the resulting point cloud accuracies in the subsequent sections.

3. DATA COLLECTION

During our test, which took place at November 18th, 2007, a distance of 13 km was covered in about 35 minutes within an area in the city centre of Stuttgart at a size of 1.5 km x 2km. Figure 2 depicts this trajectory overlaid to the corresponding section of a map.

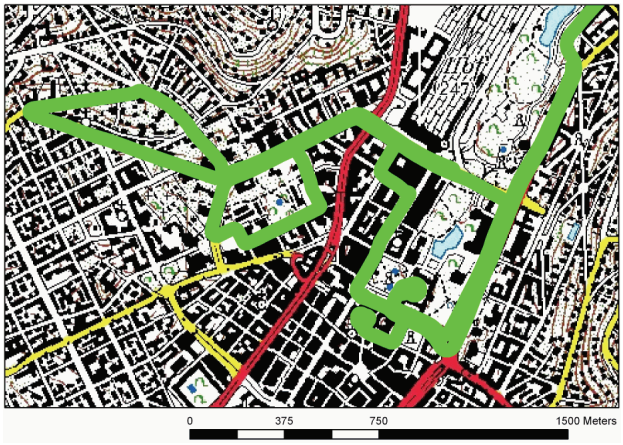

Figure 2: Trajectory covered during data collection overlaid to map of Stuttgart.

In order to investigate the presumably location dependent georeferencing accuracy of a mobile mapping system like StreetMapper area covering reference measurement are required. As an example (Barber et al 2008) used approximately 300 reference coordinates, which were measured by Real Time Kinematic GPS at corner points of white road markings. During their investigations of the StreetMapper system, these points were then identified in the scanner data due to the amplitude of the reflected pulses. Alternatively to the measurement of such singular points, which can be provided at relatively high accuracies, 3D point clouds can be measured by static TLS using standard instruments and used as reference. However, this is only feasible for selected areas due considerable effort for data collection. For this reason, our investigations are based on an existing 3D city model, which is used to provide area covering reference surfaces. A 3D visualisation of this data set is depicted together with the measured trajectory in Figure 3. This 3D city model is maintained by the City Surveying Office of Stuttgart (Bauer & Mohl, H. 2005). The roof geometry of the

respective buildings was modelled based on photogrammetric stereo measurement, while the walls trace back to given building footprints. These outlines were originally collected by terrestrial surveying for applications in a map scale of 1:500. Thus, the horizontal position accuracy of façade segments are at the centimetre level since were generated by extrusion of this ground plan. Despite the fact that the façade geometry is limited to planar polygons, they can very well be used for our purposes.

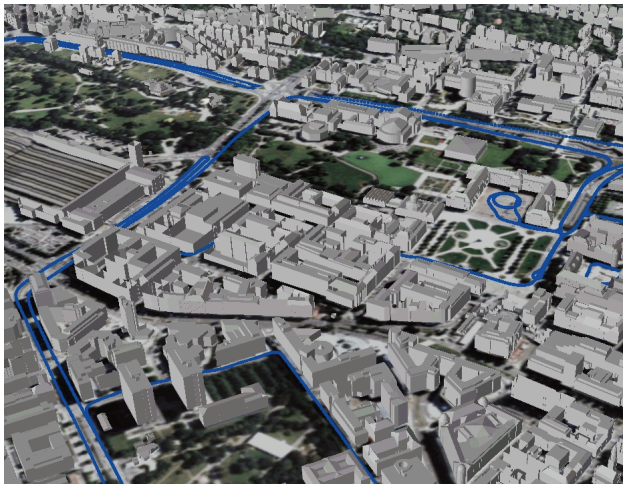

Figure 3: 3D city model used as reference data with overlaid trajectory

The quality and amount of detail for the available 3D building models as well as the collected 3D point cloud is depicted exemplarily Figure 4. This data set shows a part of the historic Schillerplatz in the pedestrian area of Stuttgart.

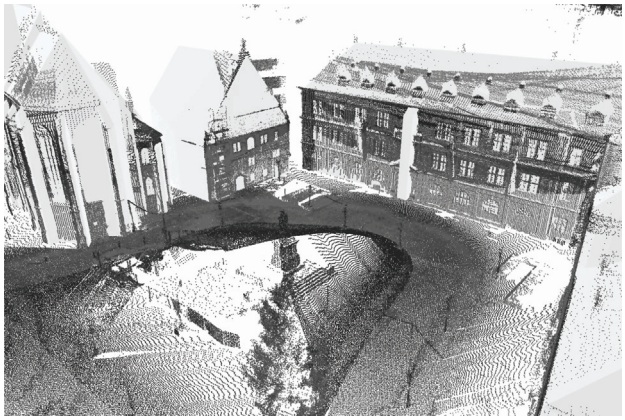

Figure 4 : Point cloud from TLS aligned with virtual city model.

4. ACCURACY INVESTIGATIONS

In order to assess the precision of the system, first the internal accuracy of GNSS/IMU processing as provided by the implemented Kalman filter will be discussed in section 4.1. In section 4.2, the available 3D building models are then used to determine the accuracy of the collected point clouds with respect to these reference surfaces.

4.1 Georeferencing accuracy

Like in airborne LIDAR, the accuracy of dynamic terrestrial LIDAR mapping from a mobile platform depends mostly on the exact determination of the position and orientation of the laser scanner during data acquisition. Nevertheless, the different conditions in a land vehicle compared to an aircraft lead to different requirements for the used GNSS/IMU system. The GNSS conditions in a land vehicle are deteriorated by multipath effects and by shading of the signals caused by trees and buildings.

Figure 5 : Measured trajectory with number of visible satellites, overlaid to DSM of test area.

These problems are clearly visible in Figure 5 which depicts the number of satellites as observed during our test. In addition to the colour coded trajectory, a grey value representation of the respective Digital Surface Model is depicted in the background of the figure in order to present the topographic situation of the test area. As it is visible, rather large areas of missing GNSS occur at very narrow streets. These areas were mainly situated in a pedestrian area, were the GNSS signal was additionally shaded by a number of trees.

Figure 6 : Estimated horizontal accuracy of the trajectory after GNSS/IMU post processing.

The applied high precision navigation system TERRAcontrol, IGI, uses the NovAtel OEMV-3 card from NovAtel Inc, Calgary, Canada. In the standard configuration the StreetMapper uses GPS and GLONASS. For the project described within this paper, only GPS was operated. Since the system is optimized for data processing in the post processing mode, the real time correction, which would be available from OmniStar HP are not used. For position and attitude determination the TERRAcontrol GNSS/IMU system is using the IGI IMU-IId (256Hz) fiber optic gyro based IMU. This Inertial Measurement Unit is successfully operated with a large number of airborne LIDAR systems and aerial cameras. It's angular accuracy of below 0.004° for the roll and pitch angle cannot be fully exploited for the short scanning distances in this application. However, the high accuracy strongly supports the position accuracy in areas of weak or missing signal of the Global Navigation Satellite System. To gain a better aiding of the inertial navigation system during periods of poor GNSS, the

GNSS/IMU navigation system for the StreetMapper is extended by an additional speed sensor. Among other benefits in the processing of the navigation data, the speed sensor slows down the error growth in periods of missing GNSS, like in tunnels or under tree cover.

For mobile mapping applications, the distance between the scanner and the measured object is typically some ten meters, compared to several hundred meters for airborne laser scanning. Therefore the contribution of the GNSS positioning error to the overall error budget is much larger than the contribution of the error from the attitude determination. Figure 6 gives the horizontal positioning accuracy which could be realised by GNSS/IMU post processing using the TERRAoffice software. As it is visible, under good GNSS conditions, an accuracy of the trajectory of about 3cm could be realized. For difficult conditions, where the GPS signal is shaded over larger distances, the error increases to some decimeters. However, despite the very demanding scenario it still can be kept below 1m.

4.2 Point cloud accuracy

In order to investigate the overall error of the final 3D point cloud, suitable reference surfaces were selected semi-automatically from the available 3D city model.

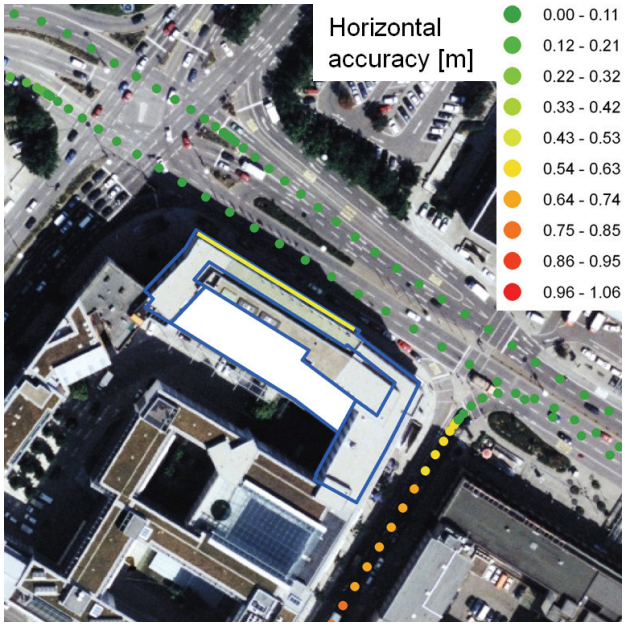

Figure 7: Ortho image with measured trajectory, selected building and part of the facade overlaid.

Figure 7 shows the ortho image for a part of our test area. The footprint of a building model, which was selected as reference object is overlaid as a blue polygon. From this building model a façade segment is again selected, which is marked as yellow line. In correspondence to Figure 6 point symbols are again used to show the trajectory of the StreetMapper system during scanning. The respective georeferencing accuracy, which was provided by GNSS/IMU processing, is represented by colour coding. Since the street in front of the selected façade is relatively broad, good GPS visibility is available for that area. This resulted in an accuracy of about 3cm for the horizontal position as provided from the Kalman filter. The points, which represent the trajectory, were generated for time intervals of 1sec, clearly showing the process of slowing down and acceleration of the vehicle.

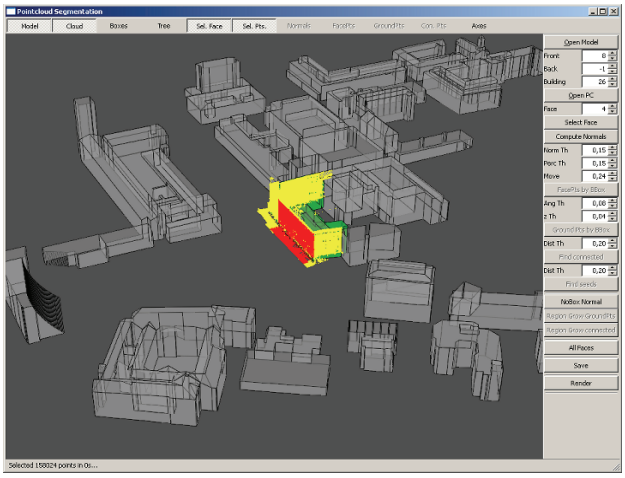

Figure 8 : 3D city model with selected reference building and corresponding section of measured 3D point cloud.

In Figure 8, the same area as already shown in Figure 7 is represented by a 3D visualisation. Figure 8 is provided from a screenshot of our GUI, which was used to select suitable reference buildings for the measured point clouds. For this purpose, the available 3D city model is visualised. The user then can interactively select single buildings and building facades. The relevant 3D point measurements can be extracted automatically by a simple buffer operation. Within Figure 8, the available LiDAR points for the building are marked in yellow, while measurements corresponding to the selected façade are marked in red and the selected building is highlighted in green.

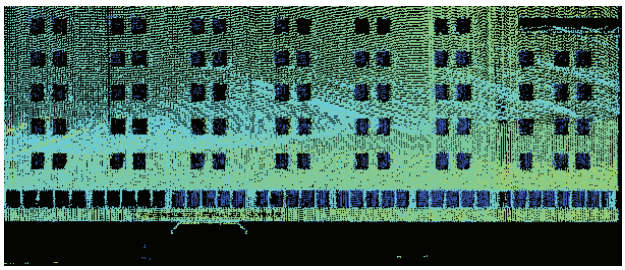

Figure 9 : Color-coded vertical distances of the measured 3D point cloud with respect to the corresponding façade surface.

After the selection process, the respective façade points are transformed to a local coordinate system as defined by this façade plane. The result of this process is given in Figure 9. There the vertical distances of the LiDAR measurements are represented as colour coded points. The façade was measured during 2 different epochs, which is also visible from the depicted trajectory in Figure 7. For our configuration a point spacing of approximately 4cm was realized. Such measurement can for example be used to provide geometric façade structure like windows and doors for the respective building model as discussed in (Becker & Haala 2007). In order to determine the accuracy of the measured LiDAR points, planar surface patches were estimated by least squares adjustment, which could then be compared to the given façade polygon from the city model. For the points depicted in Figure 7 a shift between the estimated and the reference plane of -13.8cm was determined, the standard deviation of the LiDAR points was 5.3cm. Since the horizontal accuracy of the given building façade is in the order of several centimeters, the shift between the planes can result both from errors in the LiDAR measurement and the reference model. However, the standard deviation of the points seem relatively large.

4.3 Investigation of separate scans

In order to allow a further investigation, additional features like the measured range, the look angle both with respect to the sensor platform and the reference façade, the respective scanner and the time of measurement were made available for the collected 3D point measurements. This is feasible since the StreetMapper provides the 3D point cloud in the ASPRS LAS format (Graham 2005). Based on the time of measurement and the scanner ID, the complete point cloud as depicted in Figure 9 was separated.

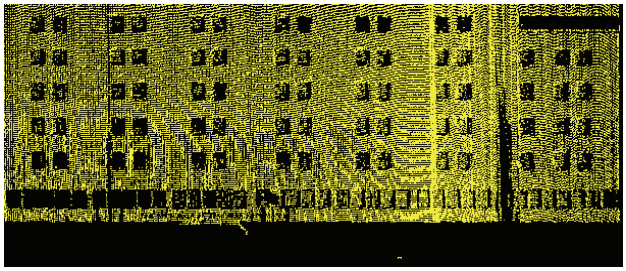

Figure 10: Points from left scanner (1), measured in epoch 1 at mean range of 41m.

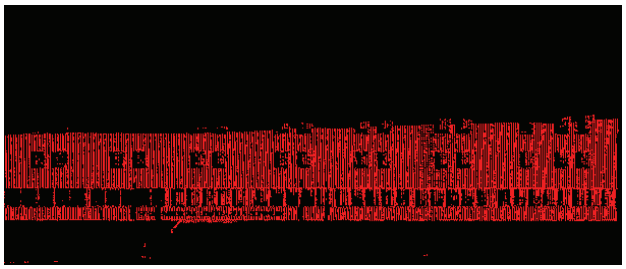

Figure 11: Points from right scanner (4), measured in epoch 2, at a mean range of approximately 15m.

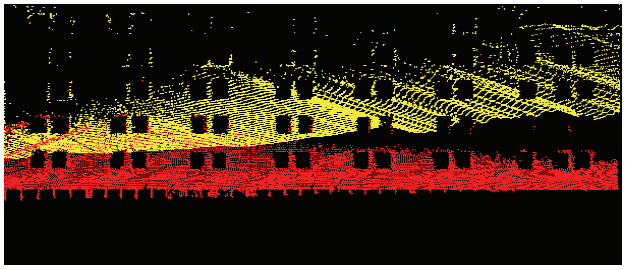

Figure 12: Points from upwards looking scanner (3). Measurements in epoch 1 (yellow) and 2 (red) at a mean range of 47m (1) and 22m (2).

Figure 10 shows the points measured by the left scanner (1) during the first pass of the vehicle (epoch 1). For these measurements, the perpendicular distance between the vehicle and the building façade was approximately 25m, resulting in a mean value of the measured ranges of about 41m. The measurements from the right scanner during the second pass of the vehicle are given in Figure 11. Due to the shorter distance between vehicle and the building, only the lower part of the façade was captured. Figure 12 depicts the measurements from the scanner looking in the upward direction. This scanner enabled point measurements at the façade for both passes of the vehicle. After separation of the respective point clouds, again planar patches were estimated and compared to the façade surface. These results are summarized in Table 1.

Scanner	Epoch	Shift [cm]	Std.dev. [cm]
1+2+3	1+2	-13.8	5.3
1	1	-13.5	0.5
2	2	-12.6	1.3
3	1+2	-15.4	5.1
3	1	-25.7	0.8
3	2	-0.08	0.5

Table 1: Estimated planes, separated for different scanners and measurement epochs.

The first line of Table 1 shows the result, if measurements from all scanners (1+2+3) at all epochs (1+2) are combined This results in a relatively large standard deviation of 5.3cm. As already discussed in section 4.2, the shift between the measured plane and the reference façade of 13.8cm is in the order of the available quality of the building model. For perfect georeferencing and system calibration, no differences between the measurements from different scanners at different epochs should be visible. However, the colour coded vertical distances for all available points already depicted in Figure 9, apparently show some systematic effects. These effects are verified by the further values in Table 1. The second row gives the result for the estimation of an adjusted plane for the points from scanner 1, period 1 (Figure 10). This resulted in a distance of -13.5cm with respect to the given façade at a standard deviation of 0.5cm. These measurements fit very well to the points from scanner 4, period 2 (Figure 11), which resulted in a shift of -12.6cm at a standard deviation of 0.5cm. However, if data from scanner 3 for periods 1 and 2 is examined, the shift is -15.4cm at a relatively large standard deviation of 5.1cm. If the data from scanner 3 are separated for epoch 1 and epoch 2, respectively, the shift is -25.7cm (epoch 1) and -0.08cm (epoch 2) at standard deviations of 0.8cm and 0.5cm. The measurements from scanner 1 and 2, which were captured at different epochs result in a difference between the estimated planar patches of just 0.9cm. This fit indicates a suitable georeferencing accuracy for epoch 1 and 2 and a good calibration of both scanners. Thus, the differences of the estimated planes to the reference plane apparently result from the error in the given 3D building model.

In contrast, the estimated planar patches from the measurements of scanner 3 show differences for epoch 1 and 2. However, the mean value of both planes again fits to the values as determined for scanners 1 and 2. The opposite signs of the deviations for scanner 3 with respect to the different driving directions apparently result from an improper boresight calibration of this instrument. These effects were verified for other building facades. In general, such calibration problems are well known from the processing of airborne LiDAR and can be solved by suitable post processing.

4.4 Long range measurements

As already discussed, the limited distance between the scanner and the measured object usually limits the contribution of the error from the attitude determination to the overall point measurement accuracy. However, in order additionally detect potentially orientation dependent errors, our investigations were repeated for a building façade measured at larger ranges. This situation is depicted in Figure 13 by the respective ortho image and the corresponding 3D visualization. In this configuration points were measured at a mean range of about 75m for scanner 1 and of 98m for scanner 4. Due to the relatively large distance to the object no measurements were available from the upwards looking scanner. Of course, larger object distances also limit the available point density at the respective facades.

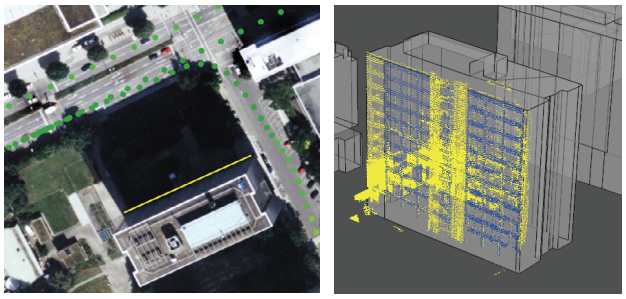

Figure 13 : Scenario for large distance measurement with ortho image (left) and selected 3D points for the respective building model (right).

Scanner	Epoch	Shift [cm]	Std.dev. [cm]
1	2	-34.8	3.2
2	1	-43.6	4.4

Table 2 : Estimated planes for large distance measurements

The test results for this scenario are given in Table 2. Despite the increasing error of the measured LiDAR points the differences between the estimated planes remain smaller than 9cm, while the standard deviation is in the order of 4cm.

4.5 Shaded GPS conditions

As it is already visible in Figure 5 and Figure 6, for some areas the shading of the GNSS satellites results in a georeferencing error up to 1m for the horizontal position. Despite the limited quality of the absolute position in the mapping coordinate system, such 3D point measurements during bad GPS conditions are still useful, especially if mainly their relative position is exploited.

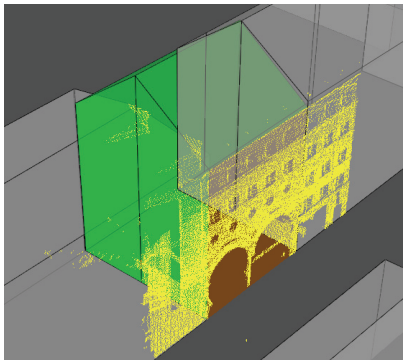

Figure 14: Captured point cloud for bad GPS conditions.

For the example given in Figure 14, rather large differences between the reference building and the estimated plane occurred to long term GPS shading in that area. Still, the standard deviation of the estimated planes is 5cm if points from the left and upward looking scanner are combined and 2.6cm if the points are separated for each scanner. For this reason, the collected point cloud can still be used for applications like precise distance measurements or the extraction of features of interest like windows or passages, if a certain error for their absolute position is acceptable.

Furthermore, the absolute accuracy of the georeferencing process can be improved, if the existing building model is used as control point information. This can be realised by an registration of the measured 3D point cloud to the given 3D building model by an iterative closest point (ICP) algorithm as presented in (Böhm & Haala 2005).

5. CONCLUSION

Within the study, the feasibility of the StreetMapper system to produce dense 3D measurements at an accuracy level of 30mm in good GPS conditions has been demonstrated. Under these good conditions remaining differences between the point clouds from different scanners can be traced back to an imperfect boresight calibration of the upward looking scanner, which can be corrected during post processing. In general, StreetMapper system provides a good and accurate coverage of 3D points at urban areas, which is practical for many mapping applications. As an example, the data can very well be used for the extraction of geometric features like windows or doors for the captured building facades.

6. REFERENCES

Barber, D., Mills, J. & Smith-Voysey, S. [2008]. Geometric validation of a ground-based mobile laser scanning system . *ISPRS Journal of Photogrammetry and Remote Sensing* **63**(1, January 2008), pp.128-141 .

Bauer, W. & Mohl, H. [2005]. Das 3D-Stadtmodell der Landeshauptstadt Stuttgart. In: Coors V. & Zipf A.e. (eds.), *3D-Geoinformationssysteme: Grundlagen und Anwendungen* Wichmann Verlag.

Becker, S. & Haala, N. [2007]. Combined Feature Extraction for Façade Reconstruction. Proceedings Workshop on Laser Scanning - LS2007 .

Böhm, J. & Haala, N. [2005]. Efficient Integration of Aerial and Terrestrial Laser Data for Virtual City Modeling Using LASERMAPS. IAPRS Vol. 36 Part 3/W19 ISPRS Workshop Laser scanning 2005 , pp.192-197.

Graham, L. [2005]. The LAS 1.1 standard. *Photogrammetric Engineering and Remote Sensing* **77**(7), pp.777-780.

Grejner-Brzezinska, D., Li, R., Haala, N. & Toth, C. [2004]. From Mobile Mapping to Telegeoinformatics: Paradigm Shift in Geospatial Data Acquisition, Processing, and Management. *PE&RS* **70**(2), pp.197-210.

Kremer, J & Hunter, G. [2007]. Performance of the StreetMapper Mobile LIDAR Mapping System in “Real World” Projects . Photogrammetric Week '07, pp. 215-225.